

## THERMAL EFFICIENCY OF SOLID ELECTROLYTE FUEL CELLS WITH MIXED CONDUCTION

P. N. ROSS, Jr.\* and T. G. BENJAMIN

Power Systems Division, United Technologies Corporation, South Windsor, Connecticut 06074 (U.S.A.)

(Received October 13, 1976; in revised form December 10, 1976)

### Summary

The effect of mixed anionic and *n*-type electronic conduction in solid electrolytes on the thermal efficiency of a fuel cell system was analyzed quantitatively. The mixed conduction observed when electrolytes based on ceria are used in H<sub>2</sub>/air fuel cell applications lowers the maximum attainable cell thermal efficiency to below 40%. Neither the zirconia nor the ceria based solid oxide electrolytes studied to date can be used in a low temperature (700 °C) system that meets simultaneously the requirements of power density and thermal efficiency for electric utility power plants. The material properties required for an advanced fuel cell power plant solid electrolyte were derived in terms of the ionic conductivity and the Schmalzried parameters  $P_{\oplus}$  and  $P_{\ominus}$ :  $\sigma_{\text{ion}} > 0.033 (\Omega\text{-cm})^{-1}$ ,  $P_{\oplus} > 10^3 \text{ atm.}$ ,  $P_{\ominus} < 10^{-28} \text{ atm.}$  at 700 °C.

---

### Introduction

Many solid oxide systems have been considered for application as oxide ion conducting electrolytes in high temperature fuel cells. Solid electrolytes of the doped zirconia type have been shown to be suitable for certain fuel cell applications [1 - 3]. They are purely ionic conductors over wide ranges of temperature and oxygen partial pressures but high temperatures (~900 °C) are required to obtain useful conductivities and the high temperatures severely limit the materials which can be used in fuel cell fabrication. The doped cerium oxides have been shown to exhibit high ionic conductivities at lower temperatures (700 °C). However, recent studies [4 - 6] have reported that doped cerias are reduced in low oxygen partial pressure atmospheres such as at the fuel cell anode and significant electronic (*n*-type) conduction may result when doped cerias are used as fuel cell electrolytes. One of the conse-

---

\*To whom correspondence should be addressed. Present address: United Technologies Research Center, Silver Lane, East Hartford, CT 06108 (U.S.A.)

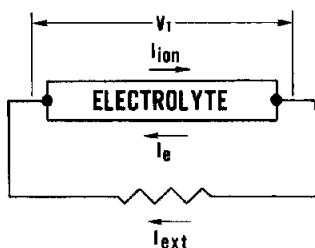


Fig. 1. Equivalent circuit for mixed-conducting solid electrolyte.

quences of mixed conduction is consumption of fuel even at zero total current to compensate for the current drain by electronic conduction, *i.e.* the cell efficiency will be reduced. The deleterious effect of mixed (ionic and electronic) conduction on the *thermal* efficiency of a fuel cell system has not been determined quantitatively for any of the ceria electrolytes. Calculation of thermal efficiency will determine whether any of the doped-ceria studied to date will meet the Electric Power Research Institute (EPRI) heat rate for advanced power plants, 7500 Btu/kWh [7] or an overall system thermal efficiency of 45.5%. The thermal efficiency defined by the power generation industry is the ratio of the power delivered to the standard enthalpy of combustion of the fuel and should be distinguished from the efficiency used by electrochemists which is the voltage efficiency, usually defined as the ratio of the power delivered to the total available Gibbs free energy in the fuel.

In the present work, we report the calculations of the performances and thermal efficiencies of ceria-based solid electrolytes and determine their potential as electrolytes for advanced fuel cell power plants. The theory of mixed conduction is also used to establish the properties which a solid electrolyte must possess in order to meet the EPRI systems thermal efficiency. Following the analysis used by Patterson [8] we have chosen to characterize these material properties by the parameters introduced by Schmalzried [9],  $P_{\ominus}$ , the  $O_2$  partial pressure at which the *p*-type electronic conductivity equals the ionic conductivity, and  $P_{\oplus}$ , the  $O_2$  partial pressure at which the *n*-type electronic conductivity equals the ionic conductivity.

## Theory

The reduction of solid electrolytes results in the generation of excess electrons by



where  $V_0$  is the concentration of oxygen anion vacancies in the lattice. The electrons created by cation reduction are easily promoted to the conduction band and electronic conduction results. The solid electrolyte can be written

as an equivalent circuit as shown in Fig. 1. Wagner's theory of mixed conduction [10] can be used to derive equations which describe the voltage, current, power and efficiency characteristics of the cell shown in Fig. 1. For the purposes of this study, only losses within the electrolyte will be considered. Therefore, the anode and cathode will be assumed reversible. Also, the terminal voltage,  $V_T$ , is assumed to be equal to the difference in the electrochemical potential of the electrons at the cathode ( $\eta_3''$ ) and at the anode ( $\eta_3'$ ):

$$FV_T = \eta_3'' - \eta_3' \quad (2)$$

In Wagner's general theory, the local charge flux of species  $i$  is:

$$I_i = -A(\sigma_i/Z_i F)\nabla\eta_i; i = 1, 2, 3 \quad (3)$$

where  $\sigma_i$  is the partial conductivity,  $Z_i$  is the valence, and  $\nabla\eta_i$  is the electrochemical potential gradient of  $i$ . In order to obtain  $\eta_1$  (cations) and  $\eta_2$  (anions), which are not experimentally measurable in terms of  $\eta_3$  (electrons) and  $\mu_{O_2}$ , the chemical potential of molecular oxygen in the gas phase, further assumptions must be made. Local equilibrium is assumed between neutral atoms, ions, and electrons. Virtual stoichiometry is assumed and the Gibbs-Duhem relation between neutral metal atoms and oxygen anions in the electrolyte is applied. Under these conditions, eqn. (3) reduced to:

$$I_{ion} = -A\sigma_{ion}(\nabla\mu_{O_2}/2Z_2F + \nabla\eta_3/Z_3F) \quad (4)$$

where

$$I_{ion} = I_1 + I_2 \text{ and } \sigma_{ion} = \sigma_1 + \sigma_2$$

Also,

$$I_e = I_3 = -A\sigma_3\nabla\eta_3/Z_3F \quad (5)$$

The system is further assumed to be at steady state so that all currents are independent of location in the electrolyte. Following Choudhury and Patterson [11] we define a current parameter,  $r$ , also independent of location in the electrolyte,

$$r \equiv I_{ion}/I_e \quad (6)$$

At fixed values of  $\mu_{O_2}''$ ,  $\mu_{O_2}'$ , each value of  $r$  defines a unique set of  $V_T$  and  $I_{ext}$ . With the assumptions of steady state and only electrolyte polarization, expressions for  $V_T$  and  $I_{ext}$  can be written in terms of  $r$ , the conductivities, and the chemical potentials. Combining eqns. (2), (4), (5), (6) with  $Z_3 = -1$  results in

$$V_T = \int_{\mu_{O_2}'}^{\mu_{O_2}''} \frac{\sigma_{ion}}{r\sigma_3 - \sigma_{ion}} \frac{d\mu_{O_2}}{2Z_2F} \quad (7)$$

The external current  $I_{ext}$  is simply the sum of  $I_{ion}$  and  $I_e$ , so eqns. (4), (5) and (6) are used to obtain:

$$I_{\text{ext}} = \frac{-A}{t} \int_{\mu_{\text{O}_2}}^{\mu_{\text{O}_2}''} \frac{[1+r] \sigma_{\text{ion}} \sigma_3}{(r\sigma_3 - \sigma_{\text{ion}})} \frac{d\mu_{\text{O}_2}}{2Z_2F} \quad (8)$$

where  $(t/A)$  is the thickness to area ratio (cell geometric factor) of the electrolyte. Equations (7) and (8) have analytical solutions if  $\sigma_{\text{ion}}$  and  $\sigma_3$  are written in terms of  $\mu_{\text{O}_2}$ . For an ideal gas, the chemical potential is related to the partial pressure by:

$$\mu_{\text{O}_2} = RT \ln P_{\text{O}_2} \quad (9)$$

For a mixed conductor exhibiting only excess electronic conduction and no hole conduction, the ionic and electronic conductivities are related by:

$$\sigma_{\text{ion}} = \sigma_3 (P_{\text{O}_2}/P_{\text{O}})^{1/4} \quad (10)$$

where  $P_{\text{O}}$  is the Schmalzried parameter for electronic conduction and corresponds to the oxygen partial pressure at which the ionic transference number,  $t_i$ , is equal to one-half, where:

$$t_i = \frac{\sigma_{\text{ion}}}{\sigma_{\text{ion}} + \sigma_3} \quad (11)$$

Substitution of eqns. (9) and (10) into eqns. (7) and (8) allows integration of  $V_{\text{T}}$  and  $I_{\text{ext}}$ . The final results are:

$$V_{\text{T}} = \frac{2RT}{Z_2F} \ln \left[ \frac{r - (P'_{\text{O}_2}/P_{\text{O}})^{1/4}}{r - (P''_{\text{O}_2}/P_{\text{O}})^{1/4}} \right] \quad (12)$$

and

$$I_{\text{ext}} = -\sigma_{\text{ion}} \left( \frac{A}{t} \right) (V_{\text{T}} - E_{\text{th}}) \quad (13)$$

where  $E_{\text{th}}$  is the theoretical open circuit potential in the absence of mixed conduction:

$$E_{\text{th}} = \frac{RT}{2Z_2F} \ln \frac{P'_{\text{O}_2}}{P''_{\text{O}_2}} \quad (14)$$

The fuel cell power,  $P$ , is simply the product of the voltage and the current:

$$P = (V_{\text{T}})(I_{\text{ext}}) \quad (15)$$

The *voltage* efficiency,  $(\eta_{\text{V}})$ , is based on the total Gibbs free energy of the fuel, equivalent to  $I_{\text{ion}}$  times  $E_{\text{th}}$ . Therefore,

$$\eta_{\text{V}} = \frac{(V_{\text{T}})(I_{\text{ext}})}{(E_{\text{th}})(I_{\text{ion}})} = \left( \frac{V_{\text{T}}}{E_{\text{th}}} \right) \left( \frac{r+1}{r} \right) \quad (16)$$

The *thermal* efficiency,  $(\eta_{\text{T}})$ , of the cell is based on the standard enthalpy of combustion of the fuel:

$$\eta_{\text{T}} = \frac{(V_{\text{T}})(I_{\text{ext}})}{\Delta H^{\circ} \text{ of fuel electrochemically converted}}$$

$$= \frac{9.53 \times 10^{-4}}{\left[ \frac{(MW)(HHV)}{nF} \right]} V_T \left( \frac{r+1}{r} \right) \quad (17)$$

where  $MW$  is the molecular weight of the fuel (in pounds),  $n$  is the number of electrons in the oxidation step, and  $HHV$  is the higher heating value of the fuel. If only hydrogen is converted electrochemically, then:

$$\eta_T = 0.67 V_T \left( \frac{r+1}{r} \right)$$

Performance characteristics for a mixed-conducting solid electrolyte can be calculated from eqns. (12) - (15) and (17), given values for  $P_{\ominus}$  and  $\sigma_{ion}$ , by allowing  $r$  to take on all values from  $-1$  to  $-\infty$ . Alternatively, the equations can be used to determine the value of the Schmalzried parameter,  $P_{\theta}$ , required to yield the desired value of  $\eta_T$ .

## Results

As mentioned above, the EPRI goal for a solid oxide electrolyte fuel cell is a total system heat rate of 7500 Btu/kWh which is equivalent to an overall thermal efficiency of 45.5%. In order to evaluate the required properties of the electrolyte, the efficiency of the electrochemical cell alone must be separated from the total system efficiency. This separation will depend in general on the overall system design, but it is possible to establish a separation that is reasonably general. We assume a hydrocarbon fuel cell application which may: (a) oxidize the hydrocarbon directly in the fuel cell anode; (b) reform the hydrocarbon to hydrogen and carbon monoxide which is electrochemically oxidized. For the latter case, we define a reformer efficiency as:

$$\eta_R = \frac{\Delta H^\circ \text{ of H}_2 \text{ and CO consumed}}{\Delta H^\circ \text{ of fuel into reformer}} \quad (18)$$

This definition of the reformer efficiency takes into account the degree of utilization of the  $H_2$  and  $CO$  in the anode. Then the electrochemical cell thermal efficiency is defined as:

$$\eta_T = \frac{\text{d.c. power delivered by cell}}{\Delta H^\circ \text{ of H}_2 \text{ and CO consumed}} \quad (19)$$

and the inverter efficiency is, as usual,

$$\eta_I = \frac{\text{a.c. power out}}{\text{d.c. power delivered by cell}} \quad (20)$$

The overall efficiency,  $\eta$ , is then  $\eta_R \eta_T \eta_I$ .

Equations (18) and (19) are easily modified for the direct hydrocarbon fuel cell. In this  $\eta_R$  represents the product of the mole fraction of the hydro-

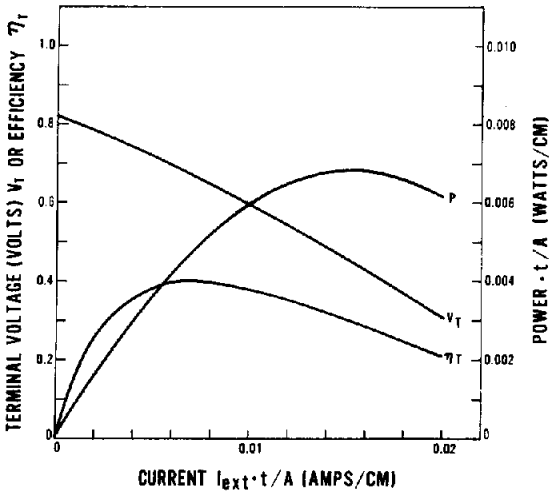


Fig. 2. Performance characteristics of  $(\text{CeO}_2)_{0.82}(\text{Gd}_2\text{O}_3)_{0.18}$  with mixed conduction at  $700^\circ\text{C}$ , air at cathode and  $P_{\text{H}_2\text{O}}/P_{\text{H}_2} = 4$  at anode,  $\sigma_{\text{ion}} = 0.033 \text{ (ohm}\cdot\text{cm)}^{-1}$ .

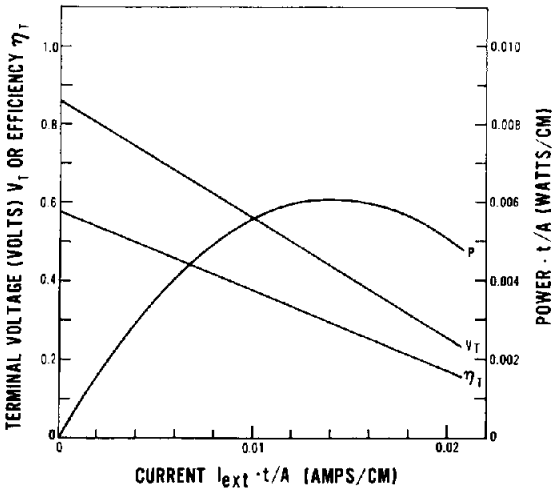


Fig. 3. Performance characteristics of  $(\text{ZrO}_2)_{0.93}(\text{Y}_2\text{O}_3)_{0.07}$  with mixed conduction at  $820^\circ\text{C}$ , air at cathode and  $P_{\text{H}_2\text{O}}/P_{\text{H}_2} = 4$  at anode,  $\sigma_{\text{ion}} = 0.033 \text{ (ohm}\cdot\text{cm)}^{-1}$ .

carbon that can be electrochemically converted and the degree of utilization of the fuel, or:

$$\eta_R = \frac{\Delta H^\circ \text{ of hydrocarbon consumed}}{\Delta H^\circ \text{ of fuel into system}} \quad (21)$$

Using reasonable values for  $\eta_R$  and  $\eta_I$  and  $\eta = 45.5\%$  the required value for  $\eta_T$  is at least 50% even for a direct hydrocarbon oxidation fuel cell.

For the sake of convenience, and comparison with experiment, pure  $\text{H}_2$  will be used as the fuel. Since reversibility is assumed for the electrodes, the

TABLE 1

Maximum thermal efficiencies at constant ionic conductivity.

System	Ref.	$T$ ( $^{\circ}\text{C}$ )	$P_{\ominus}$ (atm.)	$P \cdot (t/A)$ (W/cm)	$\eta_T$ (%)
$(\text{ZrO}_2)_{0.93}(\text{Y}_2\text{O}_3)_{0.07}$	12, 13	820	$7 \times 10^{-38}$	0.0028	50.0
$(\text{CeO}_2)_{0.82}(\text{Gd}_2\text{O}_3)_{0.18}$	4	700	$3.16 \times 10^{-19}$	0.0048	40.0
$(\text{CeO}_2)_{0.67}(\text{La}_2\text{O}_3)_{0.33}$	16	1040	$3.91 \times 10^{-15}$	0.0030	36.5
$(\text{CeO}_2)_{0.95}(\text{CaO})_{0.05}$	6	800	$1.00 \times 10^{-14}$	0.0051	30.0
$(\text{CeO}_2)_{0.95}(\text{Y}_2\text{O}_3)_{0.05}$	5	842	$1.13 \times 10^{-13}$	0.0050	28.0

use of  $\text{H}_2$  rather than a hydrocarbon changes only the open circuit potential and the value of  $P_{\text{O}_2}$  at the anode. It will be shown that these changes are relatively small and do not affect the conclusions made using  $\text{H}_2$  as the fuel. Kudo and Obayashi [4] have presented a complete analysis of cation reduction and the resulting ion-electron mixed conduction for  $\text{Ce}_{1-x}\text{Gd}_x\text{O}_{2-(x/2)}$ . For the composition described by  $x = 0.3$ ,  $\sigma_{\text{ion}} = 0.033 \text{ (ohm-cm)}^{-1}$  and  $P_{\ominus} = 3.16 \times 10^{-19}$  atm. at  $700^{\circ}\text{C}$  [4]. Figure 2 is a graphical representation of eqns. (12), (13), (15) and (17) for this system with air at the cathode and  $P_{\text{H}_2\text{O}}/P_{\text{H}_2} = 4$  at the anode (equivalent to 80% hydrogen utilization). The curves have been plotted using  $I_{\text{ext}} (t/A)$  so that they are independent of geometry. For comparison, Fig. 3 has been calculated for  $(\text{ZrO}_2)_{0.93}(\text{Y}_2\text{O}_3)_{0.07}$ , at a temperature ( $820^{\circ}\text{C}$ ) at which the conductivity of yttria-zirconia is the same as the ionic conductivity of gadolinia-ceria at  $700^{\circ}\text{C}$ .

One characteristic of mixed conduction in oxide electrolytes, as Figs. 2 and 3 clearly demonstrate, is that the efficiency passes through a maximum with increasing current density, the maximum being located often at very high current density. The performances and thermal efficiencies of fuel cells using different electrolytes can be compared using two different bases: (1) at constant conductivity, and (2) at constant temperature. The comparison at constant conductivity normalizes the electrochemical cells to the same power density in the absence of any electronic conduction in the electrolyte. Since the capital cost of the fuel cell system is scaled by the power density, the comparison of different oxide electrolytes at constant conductivity is equivalent to an approximately constant capital cost basis. Based on present technology for fabricating thin ( $\sim 100 \mu\text{m}$ ), impervious, ceramic layers,  $0.033 \text{ (ohm-cm)}^{-1}$  is a minimum conductivity needed to provide adequate power density ( $>200 \text{ mW/cm}^2$ ) and reasonable capital cost [14]. Table 1 gives a comparison of the results at constant conductivity for several doped cerias against yttria-zirconia and demonstrates clearly that in  $\text{H}_2$ /air fuel cell applications, none of the doped cerias can provide thermal efficiencies greater than 40%. Table 2 shows the constant temperature comparison at an advanced power plant temperature of  $700^{\circ}\text{C}$ . While lanthana doped ceria has a maximum efficiency close to 50%, the power density is too low to be of interest, and the efficiencies of the other ceria cells are far

TABLE 2

Maximum thermal efficiencies at constant temperature (700 °C)

System	Ref.	$\sigma_{\text{ion}} (\text{ohm}\cdot\text{cm})^{-1}$	$P_{\ominus} (\text{atm.})$	$P \cdot (t/A)$ (W/cm)	$\eta_T (\%)$
$(\text{ZrO}_2)_{0.93}(\text{Y}_2\text{O}_3)_{0.07}$	12, 13	0.0127	$1.00 \times 10^{-44}$	0.0015	50.2
$(\text{CeO}_2)_{0.82}(\text{Gd}_2\text{O}_3)_{0.18}$	4	0.033	$3.16 \times 10^{-19}$	0.0048	40.0
$(\text{CeO}_2)_{0.67}(\text{La}_2\text{O}_3)_{0.33}$	16	0.0014	$1.34 \times 10^{-26}$	0.00017	49.5
$(\text{CeO}_2)_{0.95}(\text{CaO})_{0.05}$	6	0.014	$1.00 \times 10^{-17}$	0.0021	35.7
$(\text{CeO}_2)_{0.95}(\text{Y}_2\text{O}_3)_{0.05}$	5	0.0103	$5.31 \times 10^{-18}$	0.0017	36.5

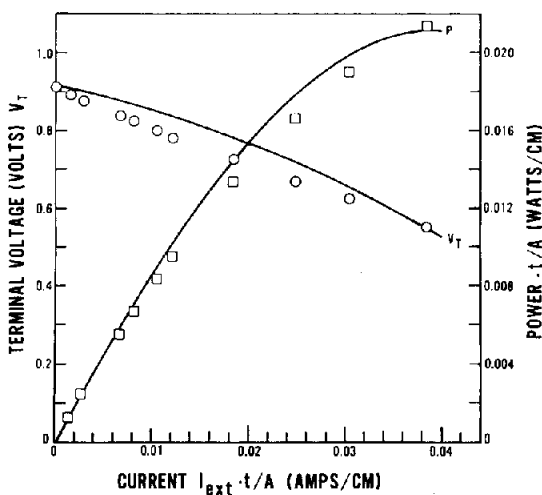


Fig. 4. Comparison of calculated and experimental performance characteristics for a gadolinia-ceria electrolyte at 715 °C, air at cathode and  $P_{\text{H}_2\text{O}}/P_{\text{H}_2} = 0.03$  at anode,  $\sigma_{\text{ion}} = 0.0672 (\text{ohm}\cdot\text{cm})^{-1}$ .

below 50%. The comparisons in Tables 1 and 2 of the performances of the yttria-zirconia cell with the doped-ceria cells clearly illustrate the severe efficiency penalty from the degree of electronic conduction occurring in doped cerias in  $\text{H}_2/\text{air}$  fuel cell applications.

One can legitimately question the validity of conclusions derived entirely from performances calculated from a theory. Performance measurements in our laboratory do confirm the essential elements in the theory of mixed conduction. Figure 4 shows a comparison of the experimental and calculated performance curves for a solid electrolyte of the ceria-gadolinia family. The values of  $\sigma_{\text{ion}}$  and  $P_{\ominus}$  measured independently for this material were  $0.0672 (\text{ohm}\cdot\text{cm})^{-1}$  and  $3.05 \times 10^{-20}$  atm., respectively. The cell configuration was:





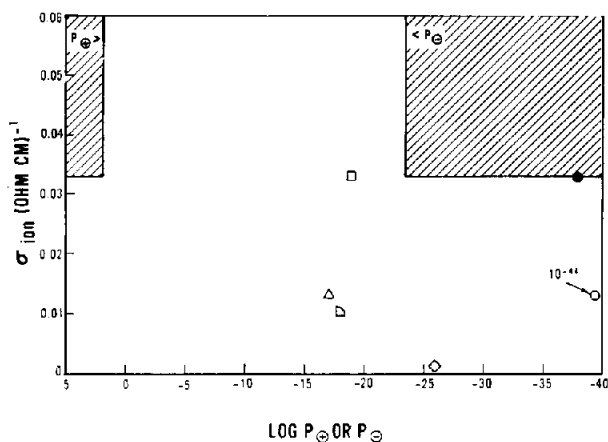


Fig. 5. Comparison of required minimum properties for oxide electrolytes (cross-hatched regions) to the observed properties of oxides at 700 °C:  $\circ$ ,  $(\text{ZrO}_2)_{0.93}(\text{Y}_2\text{O}_3)_{0.07}$ ;  $\square$ ,  $(\text{CeO}_2)_{0.82}(\text{Gd}_2\text{O}_3)_{0.18}$ ;  $\diamond$ ,  $(\text{CeO}_2)_{0.67}(\text{La}_2\text{O}_3)_{0.33}$ ;  $\triangle$ ,  $(\text{CeO}_2)_{0.95}(\text{CaO})_{0.05}$ ;  $\nabla$ ,  $(\text{CeO}_2)_{0.95}(\text{Y}_2\text{O}_3)_{0.05}$ . At 820 °C:  $\bullet$ ,  $(\text{ZrO}_2)_{0.93}(\text{Y}_2\text{O}_3)_{0.07}$ .

The close agreement between the measured and calculated performance curves adds to the validity of the analysis of potential electrolyte materials using Wagner's theory of mixed conduction.

## Discussion

Using the analysis presented here for the effect of mixed conduction on thermal efficiency, a map of the minimum properties required of oxide materials for use as solid electrolytes in  $\text{H}_2$ /air fuel cells can be drawn, as done in Fig. 5, for ambient pressure cells. It is clear that none of the materials whose properties have been reported in the literature to date meet the requirements for a low temperature (700 °C) application. The electronic conduction in the doped cerias is too high to meet efficiency requirements, and the conductivity of the doped zirconias is too low to provide both high power density (low capital cost) and high efficiency. While the map of Fig. 5 applies only to  $\text{H}_2$ /air fuel cells, the general picture is the same for a hydrocarbon fuel cell. Changing the anode gas from a  $\text{H}_2$ - $\text{H}_2\text{O}$  mixture to a  $\text{H}_2$ ,  $\text{CO}$ ,  $\text{H}_2\text{O}$ ,  $\text{CO}_2$  mixture does not result in a significant change in  $P'_{O_2}$ , since the equilibrium constant for  $\text{CO} + 0.5 \text{O}_2 \rightleftharpoons \text{CO}_2$  is very close to that for  $\text{H}_2 + 0.5 \text{O}_2 \rightleftharpoons \text{H}_2\text{O}$  for the temperature range of interest [15]. The magnitude of the component of electronic conduction is affected by the value of the ratio of  $P_{\text{H}_2\text{O}}/P_{\text{H}_2}$  in the anode, but in the practical range of usage, *e.g.* 1 to 20, the boundary for  $P_{O_2}$  in Fig. 5 is not shifted significantly.

The total system pressure affects both power density and thermal efficiency. Because the gas pressures are raised to the 0.25 power in eqn. (12),

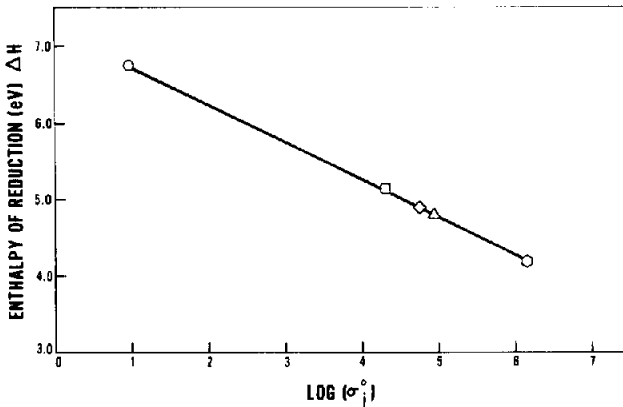


Fig. 6. Correlation between oxide reduction ( $\Delta\bar{H}$ ) and ionic conductivity ( $\sigma_i^0$ ) for:  $\circ$ ,  $(\text{ZrO}_2)_{0.85}(\text{CaO})_{0.15}$ ;  $\square$ ,  $(\text{CeO}_2)_{0.82}(\text{La}_2\text{O}_3)_{0.18}$ ;  $\diamond$ ,  $(\text{CeO}_2)_{0.95}(\text{CaO})_{0.05}$ ;  $\triangle$ ,  $(\text{CeO}_2)_{0.95}(\text{Y}_2\text{O}_3)_{0.05}$ ;  $\circ$ ,  $(\text{CeO}_2)_{0.82}(\text{Gd}_2\text{O}_3)_{0.18}$ .

substantial pressurization is required to produce any significant effect. In the case of the gadolinia-ceria electrolyte, pressurization to 100 atm. increased  $\eta_T$  from 40% to only 46%, still well below the required efficiency. For yttria-zirconia, the effect of total pressure on the power density at 700 °C for  $\eta_T > 50\%$  was examined, and it was determined that pressurization within practical limits ( $\sim 10$  atm.) did not change the power density by more than 50%, still insufficient power density for use as a low temperature solid electrolyte.

The development of a low temperature solid electrolyte fuel cell satisfying the EPRI requirements for advanced power plants hinges on the discovery of oxides having both fast anion transport and a high resistance to the creation of excess electrons at low oxygen pressure by reaction (1). There is some indication that these two properties are not independent. If we define  $\Delta\bar{H}$  as the partial molar enthalpy change for reaction (1), then the equilibrium constant,  $K$ , for this reaction will be:

$$K = K_0 \exp(-\Delta\bar{H}/RT) \quad (24)$$

Following the analysis of Kudo and Obayashi [4], it can be shown that:

$$\sigma_e = (e\mu) (K_0[V_0])^{1/2} (P_{\text{O}_2})^{-1/4} \exp(-\Delta\bar{H}/2RT) \quad (25)$$

where  $\mu$  is the electron mobility, and  $[V_0]$  the total number of oxygen vacancies in the lattice. For a fixed  $[V_0]$ , which is a function principally of the dopant level, and at a fixed  $P_{\text{O}_2}$ , the larger the  $\Delta\bar{H}$  the smaller the level of electronic conduction. If the purely ionic component of conduction is represented in the usual way:

$$\sigma_{\text{ion}} = \left(\frac{\sigma_i^0}{T}\right) \exp(-E_i/RT) \quad (26)$$

$\sigma_i^0$  is a combination of material properties such as the number of anion vacancies, the lattice parameter, and the anion jump frequency, and  $E_i$  is the activa-

tion energy for oxygen ion conduction. Our survey of the published properties of doped zirconia and doped ceria indicated that the much higher ionic conductivities in doped ceria are a result of much larger  $\sigma_i^0$  and  $\Delta\bar{H}$  for doping levels in zirconia and ceria of less than 20 a/o. At higher doping levels, no correlation was found, probably due to vacancy ordering causing deviation from the behavior predicted by eqn. (26). The correlation of Fig. 6 suggests there is a cause and effect relationship between high oxygen ion mobility in the lattice and relatively high volatility of oxygen ions from the lattice. The values of  $\Delta\bar{H}$  and  $\sigma_i^0$  required of a low temperature solid electrolyte are located in the upper right hand corner of Fig. 6, assuming that  $E_i$  is approximately 0.7 eV. It is clear that the material properties required represent a substantial deviation in material behavior from that observed in the oxides studied to date.

### Acknowledgements

The authors gratefully acknowledge the financial support of the Electric Power Research Institute (EPRI), Contract RP114, and the permission to publish this work. We thank Drs. T. Kudo and H. Obayashi of Hitachi Ltd for providing copies of their manuscripts prior to publication.

### References

- 1 Final Report, Project Fuel Cell, Research & Development Report No. 57 (1970), Office of Coal Research, Department of Interior, Washington, D.C.
- 2 E. F. Sverdrup, C. Warde and A. Glasser, in G. Sandstede (ed.), *From Electrocatalysis to Fuel Cells*, Univ. of Washington Press, Seattle, (1972), pp. 255-277.
- 3 N. Maskalick and C. Sun, *J. Electrochem. Soc.*, 118 (1971) 1386.
- 4 T. Kudo and H. Obayashi, *J. Electrochem. Soc.*, 122 (1975) 142; 123 (1976) 415.
- 5 H. Tuller and A. Nowick, *J. Electrochem. Soc.*, 122 (1975) 255.
- 6 R. Blumenthal, J. Brugner and J. Garnier, *J. Electrochem. Soc.*, 120 (1973) 1230.
- 7 Final Report to the Electric Power Research Institute, Contract RP114, Advanced Fuel Cell Technology Program, 1976.
- 8 J. Patterson, *J. Electrochem. Soc.*, 118 (1971) 1033.
- 9 H. Schmalzreid, *Z. Phys. Chem. (Frankfurt)*, 38 (1963) 87.
- 10 C. Wagner, *Z. Phys. Chem.*, B21 (1933) 25.
- 11 N. Choudhury and J. Patterson, *J. Electrochem. Soc.*, 118 (1971) 1398.
- 12 D. Swinkels, *J. Electrochem. Soc.*, 117 (1970) 1267.
- 13 J. Dixon, L. LaGrange, U. Merten, C. Miller and J. Porter, *J. Electrochem. Soc.*, 110 (1963) 276.
- 14 H. Tannenberger, in G. Sandstede (ed.), *From Electrocatalysis to Fuel Cells*, Univ. of Washington Press, Seattle, (1972), pp. 235-246.
- 15 J. Smith and H. van Ness, *Introduction to Chemical Engineering Thermodynamics*, McGraw-Hill, New York, (1959), p. 423.
- 16 T. Takahashi, K. Ito and H. Iwahara, *Proc. J. Int. d'Etudes des Piles à Combustible*, Brussels, III (1965), 42.